



OPEN

The impaired response of nasal epithelial cells to microplastic stimulation in asthma and COPD

Magdalena Paplińska-Goryca¹✉, Paulina Misiukiewicz-Stępień¹, Monika Wróbel¹, Katarzyna Mycroft-Rzeszotarska¹, Dorota Adamska², Julia Rachowka², Milena Królikowska³, Krzysztof Goryca² & Rafał Krenke¹

Microplastic particles from the air are inhaled and accumulate in the lungs, potentially causing immunological reactions and airway tissue injury. This study aimed to evaluate the biological effects of polyamide fibres on nasal epithelium co-cultivated with macrophages in control, asthma, and COPD groups. Nasal epithelial cells alone or in co-culture with monocyte-derived macrophages were exposed to polyamide fibres for 48 h. We identified 8 differentially expressed genes (DEGs) in controls, 309 DEGs in asthma (including ANKRD36C, BCL2L15, FCGBP, and IL-19), and 22 DEGs in COPD (e.g., BCL2L15, IL-19, CAPN14, PGBD5, PTPRH), particularly in epithelial/moMφ co-cultures. Microplastic exposure induced inflammatory cytokine secretion only for IL-8 production in controls (epithelial/ moMφs co-culture) and asthmatic (monoculture) epithelial cells in contrast to PM_{2.5}, which was a strong inflammatory inducer. Gene Ontology analysis revealed that microplastic exposure affected sterol and cholesterol biosynthesis, secondary alcohol metabolism, and acetyl-CoA metabolism in asthma, and cell motility, chemokine signaling, leukocyte migration, and chemotaxis in COPD. Microplastic stimulation altered the response of airway epithelial cells in obstructive lung diseases differently than in controls, linking to Th2 inflammation, stress response modulation, and carcinogenesis. Asthmatic and COPD epithelial cells are more susceptible to damage from microplastic fibre exposure.

Keywords Asthma, COPD, Epithelium, Microplastic, Pollution

Environmental pollution, including that caused by plastic derivatives, is a subject of ongoing research and active discussion. Under abiotic factors such as water, UV radiation, and biological metabolism, plastics fragment into smaller pieces: microplastics (5 mm to 1 nm) and nanoplastics (< 1 μm). Microplastics are detected in diverse aqueous ecosystems: marine water, and groundwater, agroecosystems, food, and drinking-water. Microplastic fibres present in the ambient air are released from synthetic textiles, rubber tires, or agricultural sheets. They can be inhaled as wind-driven particles from city dust and sea salt aerosols, subsequently accumulating in the lungs¹. Air derived microplastic particles typically have diameters between 7 and 15 μm with nearly 25% of fibres ranging from 100 to 500 μm in length. Studies have shown that the composition of airborne microplastics in London was dominated by polyacrylonitrile, polyester, polyamide, and polypropylene with concentrations averaging between 575 and 1008 microplastics/m²/day². The deposition of microplastics in the air is poorly understood; however, assessing their type, dosage, and correlation with weather conditions is crucial for understanding their impact on human health.

After inhalation, microplastic particles are deposited in both the upper airways by impaction and further in the small airways by sedimentation and diffusion where they have higher potential for penetration^{3–5}. The plastic fibres, with high surface area, especially thin and long particles are challenging to remove and can remain in the lungs for extended periods. Some of them are cleared from the airways with mucus and ciliary activity. Macrophages residing in the proximity of respiratory epithelium are capable of polystyrene internalization by endocytic and energy dependent pathways⁶ or by diffusion and adhesive interactions⁷. However, fibres sized between 15 and 20 μm cannot be effectively cleared by macrophages. Impaired clearance mechanisms in the airways can lead to dust overload toxicity, oxidative stress, and the expression of fibrogenic mediators, resulting in local injury. The chronic presence of plastic fibres in tissues may induce cytotoxicity and provoke responses

¹Department of Internal Medicine, Pulmonary Diseases and Allergy, Medical University of Warsaw, Banacha 1a, 02-097 Warsaw, Poland. ²Genomic Core Facility, Centre of New Technologies, University of Warsaw, Warsaw, Poland.

³Division of Optics, University of Warsaw, Warsaw, Poland. ✉email: magdalena.paplinska@wum.edu.pl

from the host's innate immunity. In vitro studies have shown that microplastic accumulation in tissues can induce oxidative stress, inflammation, as well as genotoxic effects^{8–10}.

Additionally, microplastic particles impact the lungs through their chemical and biological compounds often acting as carriers for harmful pollutants, and microbes. Particles as small as 50 nm have been shown to induce genotoxic and cytotoxic effects on pulmonary epithelial cells and macrophages cell lines¹⁰. Polystyrene microplastics contribute to pulmonary cytotoxicity by generating reactive oxygen species (ROS) and disrupting the protective pulmonary barrier by depleting ZO proteins⁸. Simultaneously, the overload of microplastic fibers triggers the airway epithelial cells and alveolar macrophages to overproduce of pro-inflammatory cytokines e.g., tumor necrosis factor alpha (TNF- α), IL-6, IL-8 potentially leading to chronic airway inflammation. Studies have demonstrated a significant correlation between elevated levels of air pollution and increased risk of mortality and morbidity, particularly in individuals with pre-existing obstructive lung diseases¹¹. Given the potential for human exposure, there is an urgent need to assess the health impacts of microplastics on the respiratory tract.

The epithelium acts as the primary interface in the respiratory tract for inhaled material, including infectious pathogens and pollutants. It protects against the harmful effects of inhaled substances through various functional mechanisms, such as trapping and clearance via the mucociliary escalator, maintaining a protective barrier with tight junctions, and initiating a local inflammatory response. Macrophages are heterogeneous cells with diverse phenotypes and polarization states. After crossing the vascular barrier in the airways, monocytes can differentiate into various macrophage populations, each located in distinct anatomical regions: bronchial macrophages, found in the bronchial walls and lumen; interstitial macrophages, residing between the alveolar epithelium and vascular endothelium, specialized in antigen presentation; and alveolar macrophages, present in the alveolar spaces adjacent to the alveolar wall. Macrophages in the airspace adhere to the epithelium and can be washed out by bronchoalveolar lavage (BAL). These cells are in direct contact with organic and inorganic particles inhaled into the lungs, with their primary function being phagocytosis and airway clearance.

This study aimed to assess the biological response of nasal epithelial cells in healthy subjects and patients with obstructive lung diseases to microplastics, specifically polyamide fibers, reported to be present in the air. The in vitro study analyzed how epithelial cells interact with immune cells present in the respiratory tract, particularly macrophages, in response to this environmental pollutant.

Materials and methods

Patient characteristics

The study involved 11 healthy controls, 10 asthma patients, and 8 patients with chronic obstructive pulmonary disease (COPD). Diagnosis of asthma or COPD in all patients was previously confirmed according to the current reports of the Global Initiative for Asthma (GINA) and the Global Initiative for Chronic Obstructive Lung Disease (GOLD), respectively^{12,13}. Inclusion criteria for asthma were: (1) the age of 18 years and older, (2) diagnosis of asthma based on past medical history, signs and symptoms of variable expiratory airflow limitation. Inclusion criteria for COPD group were as follows: (1) the age of 40 years and over, (2) diagnosis of COPD based on the past medical history, history of smoking ≥ 10 packyears, symptoms (e.g. chronic cough, exertional dyspnoea) and irreversible airway obstruction found in spirometry (z-score of the post-bronchodilator FEV₁/FVC below -1.645). The exclusion criteria included: (1) severe stages of asthma or COPD, (2) unstable or uncontrolled disease (3) a concomitant COPD and asthma diagnosis, or any other chronic or acute lung disease, autoimmune or hematological diseases, malignancies, severe cardiovascular diseases (4) treatment with systemic or nasal corticosteroids within 4 weeks before the study enrolment (5) asthma or COPD exacerbation within 3 months preceding mucosal sampling, or respiratory tract infection symptoms within the same period. The control group comprised non-smokers with normal spirometry and without symptoms of respiratory tract infection in the preceding 3 months. Clinical characteristic of the study participants is shown in Table 1. The study protocol was approved by the Ethics Committee of the Medical University of Warsaw (KB/30/2022) and all participants provided informed written consent.

Particles isolation

Microplastic fibres were prepared following a modified protocol published by Cole¹⁴. Polyamide fishing line (0.08 mm diameter) and polyamide thread (0.16 mm diameter) were aligned by wrapping them around a spool (two stable bolts), coated with a thin layer of a glycol based, water-soluble freezing agent (Bio Optica) and frozen in -80 °C for 15 min. Once frozen solid, fibers were cut into 1–2 mm pieces using a guillotine. To prevent the freezing agent from softening the fibres were periodically returned to the freezer. The fibres were suspended in ultra-pure warm water (45 °C) and centrifuged (4200 x g for 15 min, 4 °C). The fibres were then homogenized using both a mechanical (Ika) and an ultrasonic homogenizer (Branson Sonifier, Emerson) for 15 min. After homogenization, the microplastic fibres were centrifuged (4200 x g for 15 min, 4 °C), dried, weighed, UV irradiated and suspended in PBS at a concentration of 5 µg/µL. PM_{2.5} particle were obtained from the Silesian University of Technology, collected, and isolated as previously described¹⁵. The samples were (collected with a low-volume PM sampler type PNS-15 (Atmoservice) 1.5 m above the ground, at a flow rate of 2.3m³/ h in Gliwice during heating season). Daily PM_{2.5} samples were collected continuously on high-purity quartz (SiO₂) microfiber filters (QM-A Whatman) with 47 mm diameter. The filters were weighed, cut into small pieces, suspended in PBS; the particles were detached from filters by sonication, filtrated through strainers with 70 µm pores (Corning). The sediment of the particles was dried at 96 °C to dry mass, weighted, resuspended in PBS into stock solution containing 5 µg/µL PM_{2.5}, and autoclaved.

Raman spectrometry

The tested material was suspended in saline and placed on the Raman-grade CaF₂ glass which does not produce Raman signal in the relevant spectral region. The measurements were performed using an inVia confocal Raman

	Control (n = 11)	Asthma (n = 10)	COPD (n = 8)	p-value
Age (years)	39.5 (32–45) #	49 (38–67)	64 (61–68) #	0.004
Gender (F/M)	6/5	4/6	4/4	
BMI (kg/m ²)	22.6 (20.5–24.9) *#	29.5 (27.1–34) *	30 (28.6–33.3) #	0.002
Smoking exposure (pack-years)	0 (0–0) #	0 (0–0) &	16 (15–40) #&	0.03
FEV ₁ (% predicted)	104.5 (94–111) #	87.5 (76–101.5)	67 (45–88) #	0.01
z-score FEV ₁	0.089 (-0.467–0.869) #	-0.98 (-1.54–0.07)	-2.02 (-3.27 – -0.79) #	0.02
FVC (%)	108 (105–112)	98.5 (84.5–110)	109 (96–127)	0.269
z-score FVC	0.597 (0.2–0.975)	-0.14 (-1.14–0.43)	0.46 (-1.87–1.75)	0.303
FEV ₁ /VC (%)	87.1 (81.8–95) #	81.3 (70.5–92) &	49.1 (42.8–62.1) #&	0.0004
z-score FEV ₁ /VC	-0.55 (-1.10 – -0.09) #	-0.89 (-1.76 – -0.56) &	-3.275 (-4.26 – -2.64) #&	0.0006
ACT (points)	-	23 (20.5–24.5)	-	N.A.
mMRC (points)	-	-	1.5 (1–2)	N.A.

Table 1. Characteristics of study participants. Data are presented as median (IQR) or n. ACT – asthma control test, BMI – body mass index, FEV₁ – forced expiratory volume at first second, mMRC – modified Medical Research Council, N.A. – not applicable, VC – vital capacity. Kruskal-Wallis or Chi square test. *control vs. asthma; # control vs. COPD; &asthma vs. COPD.

microscope, which combines a bright-field microscope with a Raman spectrometer. A Nd: YAG laser operating at 532 nm was used as the excitation source. The system included microscope objectives with increasing magnification and a 2400 l/mm diffraction grating. Spectra were recorded in the Raman fingerprint region at a resolution 1 cm⁻¹/pixel.

Several subsamples were analyzed to assess microplastic homogeneity. Spectra were collected by positioning the laser spot on the material, under the bright-field configuration, and measuring with two parameter sets. Spectra of samples 1 and 2 were collected with 3 s exposure and 10 accumulations, while spectra of samples 3 and 4 were collected with 5 s and 20 accumulations.

Cell culture and scheme of the study

Nasal epithelial cells were isolated, cultured and differentiated as previously described¹⁵. Epithelial cells were obtained by nasal brushing (Cytobrush Plus GT, CooperSurgical). The cells were detached from the brush by gentle agitation, centrifuged (300 g, 10 min, room temperature) and treated with Accutase (BD Biosciences) for 10 min. in 37 °C. The cell pellet was suspended in a total volume of 5 ml of airway epithelial growth medium (PromoCell) containing antibiotics and seeded into T25 bottles (Thermo Fisher Scientific) and incubated for 24 h at 37 °C. The undetached cells were removed, the adhered cells were cultured until reached 80% of confluence. The cells were maintained at an air-liquid interface (ALI) for 21 days in PneumaCult medium (StemCell) within a two-chamber system with apical surface of 6.5 mm trans well Thin Certs with 0.4 µm pore size and placed in 24 well flat-bottomed plates (Greiner Bio-One). Peripheral blood mononuclear cells (PBMCs) were isolated from freshly drawn venous blood via Lymphoprep (StemCell) centrifugation. The PBMC monocytes were achieved by adherence in X-vivo 20 (Lonza) for 24 h. Monocyte derived macrophages (moMφs) were differentiated using 20 ng/ml macrophage colony-stimulating factor (M-CSF) (StemCell) over 10 days.

For this project, we developed a macrophage-epithelial co-culture model where monocyte-derived macrophages were placed on top of the epithelium, and microplastic stimulation was applied to the apical side of the epithelial cells. Co-cultures contained nasal ALI epithelial cells, and 5×10^4 of fully differentiated moMφs (cultured for 10 days before the experiment) suspended in 10 µl of macrophage medium was loaded on the top of the epithelium (Fig. 1). The co-cultures were autologous, i.e. for each co-culture, the epithelial cells, macrophages were obtained from the same individual. 200 µg/cm² microplastic fibres or 50 µg per insert of freshly prepared PM_{2.5} was added apically to epithelial cells after cells were combined in co-culture for 48 h in a scheme as follows:

- (1) Epithelial cells (monoculture)
- (2) Epithelial cells + moMφs (co-culture)

Cell viability

Cell viability was assessed by measuring lactate dehydrogenase (LDH) release, using the Cytotox96 assay (Promega) according to the manufacturer's protocol.

Transepithelial electrical resistance (TEER)

Transepithelial electrical resistance (TEER) was measured using a Millicell ERS-2 Voltohmometer (Merck Millipore) as per the manufacturer's protocol. The ohmic resistance of a blank (insert without cells) was subtracted from the total resistance and the value was normalized to the area (cm²) of the epithelial layer.

RNA isolation

After 48 h of incubation macrophages were washed out. The attached cells were collected, total RNA was isolated by TRI reagent (Sigma-Aldrich) method and further purified with NucleoSpin RNA (Machery&Nagel)

using protocol including DNA digestion. Concentration and quality of isolated RNA were determined using spectrometer (Beckman).

RNA-Seq analysis

mRNA sequencing was performed on 4 control, 4 asthmatics, and 4 COPD samples of unstimulated and microplastic-treated epithelium monocultures. Libraries for the RNA-Seq were prepared according to the manufacturer's protocol for the KAPA mRNA HyperPrep Kit (Roche). A total of 1000 ng of intact total RNA was subjected to mRNA enrichment, heat fragmentation (94 °C, 5 min), cDNA synthesis and ligation of KAPA Unique Dual-Indexed Adapters (Roche). Ten cycles of library amplification were applied. The size distribution of the final libraries was validated using an Agilent TapeStation 2200 and High Sensitivity D1000 Reagents (Agilent) and the concentration was determined by qPCR using a Kapa Library Quantification Kit (Roche). Sequencing was performed on an Illumina NovaSeq 6000 using the NovaSeq 6000 S1 Reagent Kit (Illumina), generating 2 × 100 paired-end reads using the manufacturer's standard protocols. High quality output data were obtained, with more than 95% of bases with quality exceeding Phred Score Q37 in an amount of 27–41 MR/sample.

Bioinformatic analysis

Raw sequences were trimmed according to quality using Trimmomatic¹⁶ (version 0.39) with default parameters, except MINLEN, which was set to 50. Trimmed sequences were then mapped to the human reference genome provided by ENSEMBL, (version grch38_snp_tran) using Hisat2¹⁷ with default parameters. Optical duplicates were removed using Mark Duplicates tool from GATK¹⁸ package (version 4.2.3.0) with default parameters except OPTICAL_DUPLICATE_PIXEL_DISTANCE which was set to 12,000. Reads that did not map to the reference were extracted using Samtools¹⁹ and aligned to the Silva meta-database of rRNA sequences²⁰ (version 119) using Sortmerna²¹ (version 2.1b) with “best 1” option. The mapped reads were then associated with transcripts from GRCh38 database²² (Ensembl, version 110) using HTSeq-count²³ (version 2.0.1) with default parameters except for -stranded set to “reverse”. Differentially expressed genes were identified using the DESeq2 package²⁴ (version 1.38.3). Fold change was corrected using aperglm²⁵. P-values were corrected for multiple hypothesis testing with Benjamini-Hochberg algorithm. Overrepresentation of Gene Ontology (GO)²⁶ terms and Kyoto Encyclopedia of Genes and Genomes (KEGG)²⁷ categories among the top 5% of genes (according to p-value) was assessed using the cluster profiler package²⁸. The RNA-Seq data were uploaded to GEO Omnibus (reference no. GSE273262). <https://www.ncbi.nlm.nih.gov/geo/query/acc.cgi?acc=GSE273262>.

PCR

cDNA synthesis was carried out with 1 µg of total RNA using the High Capacity cDNA Reverse Transcription Kit with RNase Inhibitor (Thermo Fisher Scientific). Quantitative real time PCR was performed to assess the mRNA expression of 11 genes selected from RNA-Seq analysis: PTPRH (Hs00936202_m1), C15orf48 (Hs00260902_m1), BCL2L15 (Hs01017582_m1), CAPN14 (Hs00871882_m1), MAFF (Hs05026540_g1), ANKRD36C (Hs00923115_m1), FST (Hs01121165_g1), IL19 (Hs00604657_m1), PKP1 (Hs00240873_m1), FCGBP (Hs00175398_m1), PGBD5 (Hs00226116_m1) and 18s rRNA (Hs99999901_s1) in epithelial cells. The quantitative real time PCR analysis was performed on an ABI-Prism 7500 Sequence Detector System (Applied Biosystems). Relative quantification values were calculated using the $2^{-\Delta\Delta CT}$ method with 18s rRNA serving as an internal control to normalize gene expression levels. Unstimulated epithelial cells from epithelial monocultures of each individual were used as a calibrator.

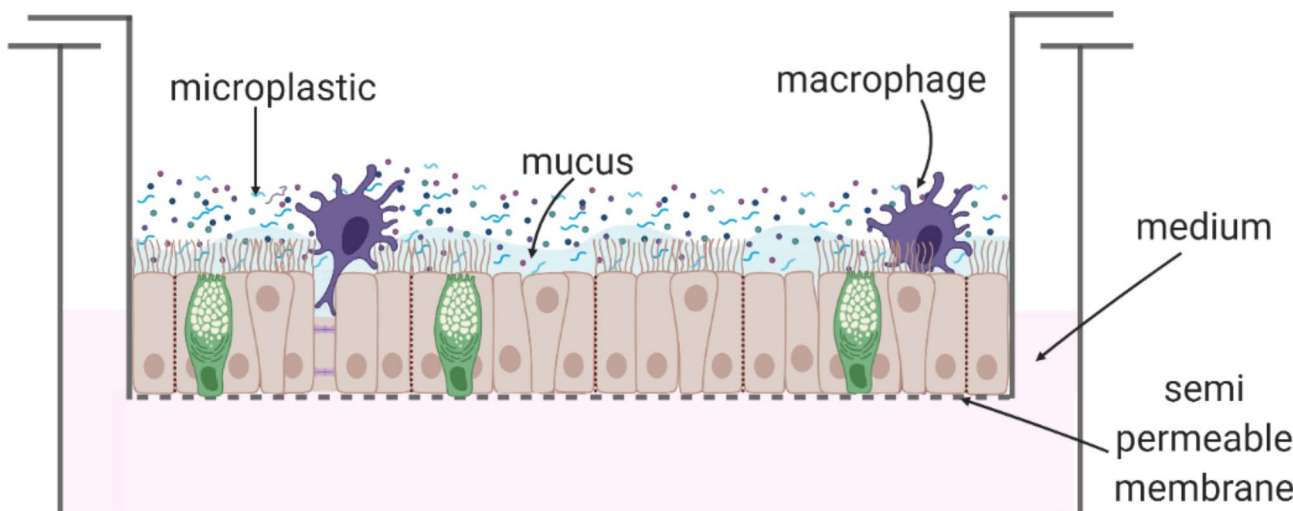


Fig. 1. The scheme of the epithelial- moMφs co-culture used in the study.

ELISA

The levels of IL-1 β , IL-6, IL-8 were measured using ELISA (Thermo Fisher Scientific) according to the manufacturer's protocol. The sensitivity of ELISA kits was 2 pg/ml.

Flow cytometry

We used CD49f, β -Tubulin, TSPAN as markers for epithelial subtypes based on our previous experience and literature data²⁹. The expression of tetraspanin-8 (TSPAN8) is upregulated in mucin-secreting cells in our study is used as a marker of secretory epithelial cells^{30,31}. It was shown that TSPAN8 expression in airway secretory cells was higher than in basal cells and comparable to two secreted mucins, MUC5AC and MUC5B. This marker is localized in plasma and regulates the release of mucin granules during the slow and sustained phase of ATP-stimulated secretion. Alpha-6 integrin (CD49f) is a well described marker of basal epithelial cells, often used as a selective marker for stem and progenitor cells from monolayer cultures³². β -tubulin together with α -tubulin are a main component of microtubules, cilia of epithelial cells are rich in tubulin - this protein is a marker for ciliated epithelial cells. In this study we evaluated the effect of microplastic on epithelial biology processes. We evaluated the possible microplastic impact associated with remodeling (EGFR, TGF- β)³³, Th2 immunity (CD193)³⁴ and cancer (CD24 –frequently described as a marker for cancer prognosis and therapy, its role was described in tumour growth, invasion and metastasis)³⁵.

The cells were rinsed with PBS (without Ca^{2+} and Mg^{2+}) and detached with Accutase (BD Biosciences) for 15–20 min. In macrophage cultures the undetached cells were scraped with cell scraper (Corning). The Accutase was neutralized with fresh medium, cells were centrifuged (200 x g, 20 °C, 10 min) and suspended in Stain Buffer (FBS) (BD Biosciences). Epithelial cells were stained with antibodies against the surface binding molecules: Tetraspanin-8 (TSPAN8) (BV786, rat anti-human cat. no. 748226), CD49f (BV650, rat anti-human, cat. no. 563706), epidermal growth factor receptor (EGFR) (BV421, mouse anti-human, cat. no. 566254), CD193 (BB700, mouse anti-huma, cat. no. 745843), CD45 (APC-H7, mouse anti-human cat. no. 641408) (BD Biosciences), CD24 (BV510, mouse anti-human cat. no. 563035) (BD Biosciences), in BD Horizon Brilliant Stain Buffer (BD Biosciences). The cells were incubated for 20 min in the dark at room temperature. After washing away, the reagents, the cells were fixed and permeabilized using lysis buffer and permeabilizations solution 2 (BD Biosciences), then stained with intracellular marker: β -tubulin (Alexa Fluor 488 mouse anti- α -Tubulin, cat. no. 322588, Invitrogen, Thermo Fisher Scientific) and Transforming Growth Factor beta-1 (TGF- β) (PE, mouse anti-human, cat. no. 562339, BD Biosciences,) for 20 min in the dark.

For macrophages, BD Pharminge Human BD Fc Block (BD Biosciences) (5 μl per 100 μl of sample) was added to block non-specific bindings. Macrophages were then stained with antibodies against the following surface binding molecules: Toll-like receptor 4 (TLR4) (BV605, mouse anti-human, cat. no. 743692), CCR2 (R718, mouse anti-human cat. no. 751973), CD210A (PE, rat anti-human cat. no. 556013), HLA-DR (APC, mouse anti-human cat. no. 641402), CD44 (BV510, mouse anti-human cat. no. 744268), CD206 (PE-CF594, mouse anti-human cat. no. 564063), CD14 (Alexa Fluor 488, mouse anti-human cat.no. 562689).

Cells were analysed by flow cytometry using a FACSCelesta instrument (BD Biosciences) equipped with blue (488-nm), violet (405-nm), and red (640-nm) lasers. Unstained cells and compensation beads (BD Biosciences) were used to set voltages and create single stain negative and positive controls. Compensation was adjusted to account for spectral overlap between the seven fluorescent channels used in the study. Samples were examined by side scatter area (SSC-A) versus forward scatter area (FSC-A), followed by forward scatter height (FSC-H) versus FSC-A to select single cells, thereby eliminating debris and clumped cells from the analysis. Data were analyzed using FlowJo software version 10.8.1 (Tree Star).

The epithelial cell subpopulations were defined as follows:

- Epithelial cells with basal phenotype: CD49f + β -Tubulin- TSPAN-.
- Epithelial cells with secretory phenotype: TSPAN + CD49f- β -Tubulin-.
- Epithelial cells with ciliated phenotype: β -Tubulin + TSPAN-CD49f-.

The gating strategy is presented on Figure S1 (Supplementary file).

Statistical analysis

Statistical analysis was performed using GraphPad Prism (version 9.3.1). The Mann-Whitney test was applied for pairwise comparisons, while the Kruskal-Wallis test for comparisons between continuous variables across three groups. Results are presented as median and interquartile range (IQR) or 5–95 percentile. Differences were considered statistically significant at $p \leq 0.05$.

Results

Characteristics of microplastic fibres

The collected spectra were loaded and analyzed using Python code which facilitated the removal of the baseline caused by the sample's fluorescence and the preparation of spectral plots with lines marking the important Raman peaks present in the spectra (Fig. 2). The collected spectra were compared to Raman spectra of synthetic materials available in the literature^{36–38} and identified as nylon due to the characteristic peaks of amides, with the most intense peak being the C=O stretch of Amide I at 1636 cm^{-1} . Amide II can be identified by the C-N stretch and N-H bend at 1467 cm^{-1} ³⁸. Peaks at 1062, 1078 and 1126 cm^{-1} were assigned to the C-C skeletal stretching, while bands at 1308, 1370, 1442 cm^{-1} corresponded to the twisting, wagging and bending modes of CH₂, respectively^{38,39}. The peak at 931 cm^{-1} results from the C-CO stretching mode and the peak at 1480 cm^{-1} can be attributed to CNH bending^{38,39}. The doublet at $\sim 1300 \text{ cm}^{-1}$ can be attributed to CH₂ and its high intensity in the measured spectra may be caused by the specific symmetry species of the measured sample⁴⁰. All collected

spectra were similar confirming sample homogeneity. Based on comparison with Raman spectra of synthetic materials in the literature, the analyzed material was identified as polyamide (nylon).

Cytotoxicity of polyamide fibres

Polyamide fibers did not cause cytotoxic effects after 24–48 h in any of the investigated concentrations in nasal epithelial cells (Fig. 3).

The effect of microplastic fibres on transepithelial electrical resistance (TEER) changes

As expected, asthmatic epithelial cells exhibited the lowest TEER values compared to controls and COPD (Fig. 4A), reflecting the impaired barrier integrity of the asthmatic epithelium, which is linked to the disease pathobiology. A distinct pattern of TEER changes following microplastic stimulation was observed in control and COPD epithelial cultures (Fig. 4B). In the control group, 48 h microplastic treatment decreased TEER values in epithelial/moMφ co-cultures (Δ TEER 15.4 Ω (-23–37.7 Ω)) compared to untreated epithelial/moMφ co-cultures (Δ TEER 49.6 Ω (5–72.3 Ω)). In the COPD group microplastic stimulation reduced TEER values in epithelial monocultures (Δ TEER – 25.3 Ω (-93.5–6.6 Ω)) compared to untreated epithelium (Δ TEER 9.1 Ω (-27.5–39.9 Ω)). Interestingly, microplastic treatment of COPD epithelial/moMφ co-cultures increased Δ TEER values compared to monocultures (Δ TEER 8.8 Ω (-27.8–37.7 Ω)).

RNA-Seq data analysis, selection of differentially expressed genes (DEGs) and their analysis in RT-PCR – the candidates of markers of epithelial response to microplastic stimulation in healthy, asthma and COPD groups

RNA-Seq data analysis revealed that microplastic treatment of epithelial cells resulted in 8 differentially expressed genes (DEGs) in the control group, 309 DEGs in the asthma and 22 DEGs in the COPD group. Multivariable analysis across groups identified 199 DEGs as the most significantly altered genes after microplastic stimulation (Table 2).

Nine genes with the lowest adjusted p-value and the highest (≥ 1.37) (8 genes: ANKRD36, BCL2L15, C15orf48, FST, IL-19, MAFF, PGBD5, and PTPRH) and the lowest (< 0.63) (0 genes) fold changes from multivariable analysis of RNA-Seq results, along with the three most significantly altered genes from comparisons within the control, asthma, and COPD groups (PKP1 adjusted p-value 0.001 FC = 0.76), asthma (FCGBP adjusted p-value 2×10^{-22} , FC = 1.97) and COPD (CAPN14 adjusted p-value 0.0000005, FC = 2.42) groups were selected for PCR verification in epithelial monocultures as well as epithelial/moMφs co-cultures (Fig. 5). In the asthmatic group, important markers of microplastic activity included ANKRD36C, BCL2L15, C15orf48, FCGBP, FST, IL-19, MAFF, PKP1, and PTPRH. The expression of these genes increased in both mono- and co-cultures of epithelial cells following microplastic stimulation. Notably, CAPN14 and PGBD5 showed increased expression in asthmatic epithelial monocultures but not in epithelial/moMφs co-cultures after microplastic stimulation. In the COPD group, microplastic stimulation was associated with elevated expression of BCL2L15 and IL-19 in both: mono and macrophage co-cultures of epithelial cells. However, increased expression of AKRD36, C15orf48, CAPN14, PGBD5 and PTPRH was found only in epithelial/moMφs co-cultures, while FST was upregulated exclusively in epithelial monocultures. It is noteworthy that all the aforementioned changes in mRNA expression were observed in comparison to unstimulated epithelial monocultures. The only exception was observed for C15orf48 in asthma. Its expression was higher in epithelial monoculture 2.3 fold change (1.7–3.5 fold change) and epithelial/moMφs co-culture 2.8 fold change (2.9–2.3 fold change) compared to unstimulated epithelium 1 fold change (1–1 fold change) and unstimulated epithelial/moMφs co-cultures (1.7 fold change (2.4–0.3 fold change), respectively. Interestingly, none of the analyzed markers showed significant expression changes in epithelial cells of control subjects following microplastic treatment.

Gene Ontology – analysis of biological processes impacted by microplastic in asthma and COPD epithelial cells

Gene Ontology (GO) annotation revealed significant changes in gene expression (both upregulated and downregulated) in microplastic-exposed epithelial cells from the asthma and COPD groups, associated with the 8 and 21 terms respectively, but none in the control group (Fig. 6). In the asthma group, microplastic exposure affected genes associated with the following biological processes: sterol biosynthetic process (GO:0016126, 13 genes), secondary alcohol metabolic process (GO:1902652, 19 genes), cholesterol biosynthetic process (GO:0006695, 12 genes), secondary alcohol biosynthetic process (GO:1902653, 12 genes), alcohol metabolic process (GO:0006066, 33 genes), small molecule biosynthetic process (GO:0044283, 40 genes), acetyl-CoA metabolic process (GO:0006084, 8 genes), dicarboxylic acid metabolic process (GO:0043648, 12 genes). In the COPD group microplastic exposure influenced different biological processes, with the 10 most significant terms being: positive regulation of cell motility (GO:2000147, 50 genes), chemokine-mediated signaling pathway (GO:0070098, 13 genes), response to chemokine (GO:1990868, 14 genes), cellular response to chemokine (GO:1990869, 14 genes), positive regulation of locomotion (GO:0040017, 50 genes), leukocyte migration (GO:0050900, 35 genes), cellular response to biotic stimulus (GO:0071216, 26 genes), regulation of endothelial cell apoptotic process (GO:2000351, 10 genes), chemotaxis (GO:0006935, 36 genes), taxis (GO:0042330, 36 genes).

We compared the genes associated with the GO terms significantly affected by microplastic exposition and found that ACYLY was the only common gene for selected terms in asthma. In COPD we analysed the genes associated with positive regulation of cell motility, positive regulation of locomotion, cellular response to biotic stimulus, leukocyte migration, chemotaxis, taxis, and cellular response to chemokine we found three common genes: TREM2, CXCL8, CX3CL1.

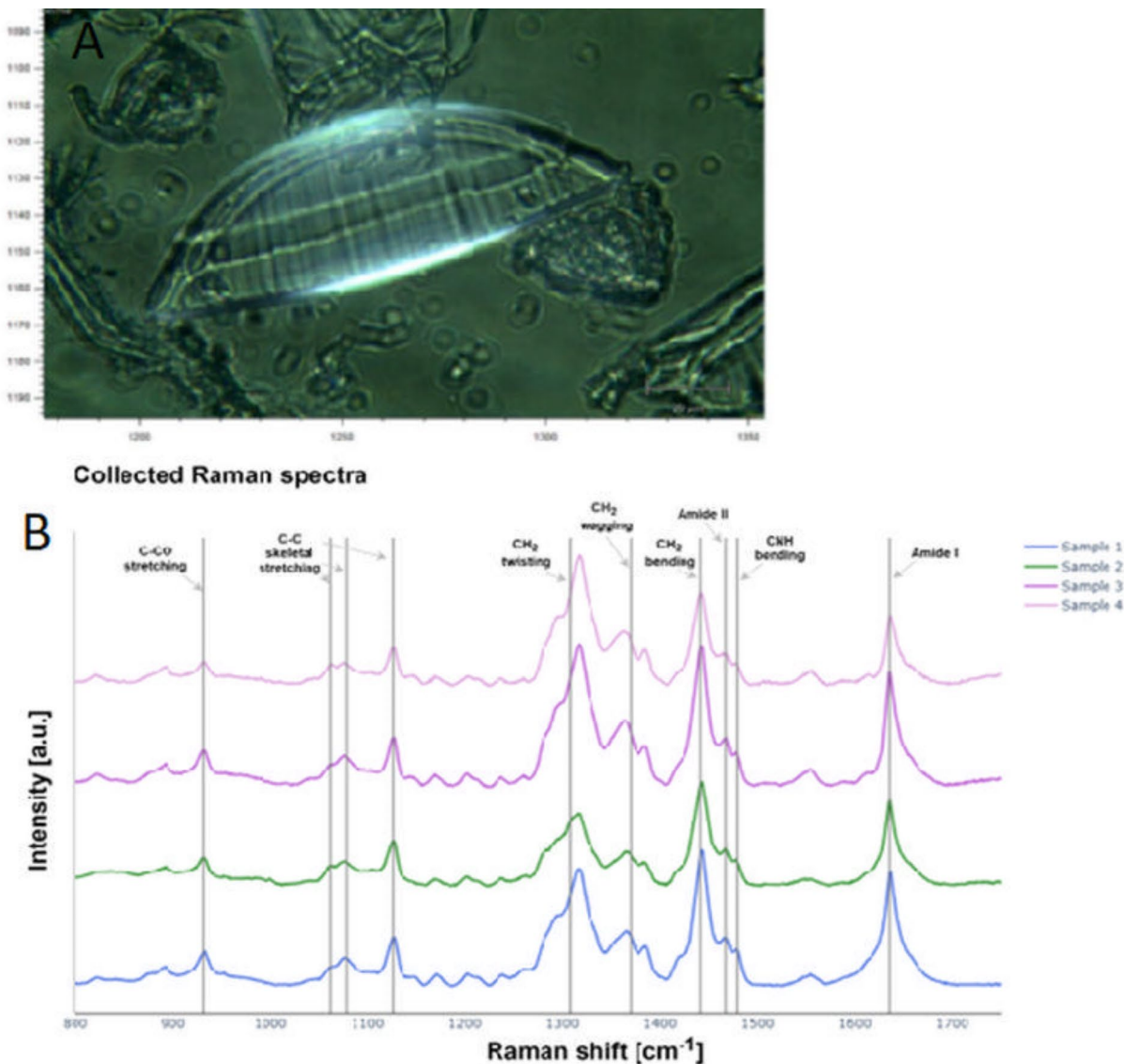


Fig. 2. Bright-field microscope image of a microplastic particle (A); Raman spectra collected for different samples. The baseline was removed, and plots were shifted vertically for clarity (B).

The effect of polyamide fibres on inflammatory cytokines' secretion by epithelial cells in control asthma and COPD groups

Epithelial cells from asthmatic patients produced higher levels of IL-1 β compared to controls and IL-6 compared to control and COPD (Fig. 7). Microplastic stimulation induced inflammatory cytokine secretion only for IL-8 production in controls (epithelial/ moM ϕ s co-culture) and asthmatic (monoculture) epithelial cells (Fig. 7). Co-cultivation with moM ϕ s did not change the epithelial response to microplastic stimulation, it decreased IL-6 level in controls and asthma groups regardless microplastic treatment. PM_{2.5} in contrast to microplastic was a strong inducer of inflammation. PM_{2.5} increased the level of IL-1 β in asthma, IL-6 in control, IL-8 in control and asthma groups.

The effect of polyamide fibres on the expression of CD24, CD193, EGFR and TGF β in control, asthma and COPD epithelial cells

Flow cytometric analysis of epithelial cells (CD45 $^-$ phenotype) revealed an increased number of CD24 $^+$ epithelial cells following microplastic treatment in the asthma group compared to controls (Fig. 8). Further analysis of basal, secretory, and ciliated epithelial cells showed that microplastic stimulation increased the number of CD24 $^+$ ciliated epithelial cells in the asthma group compared to the control group. This treatment upregulated CD193 expression on basal epithelial cells in controls compared to COPD and on secretory epithelial cells in asthma compared to COPD. Regardless of microplastic treatment, the number of EGFR $^+$ basal epithelial cells was higher in asthma compared to controls. Microplastic stimulation decreased the number of EGFR $^+$ ciliated

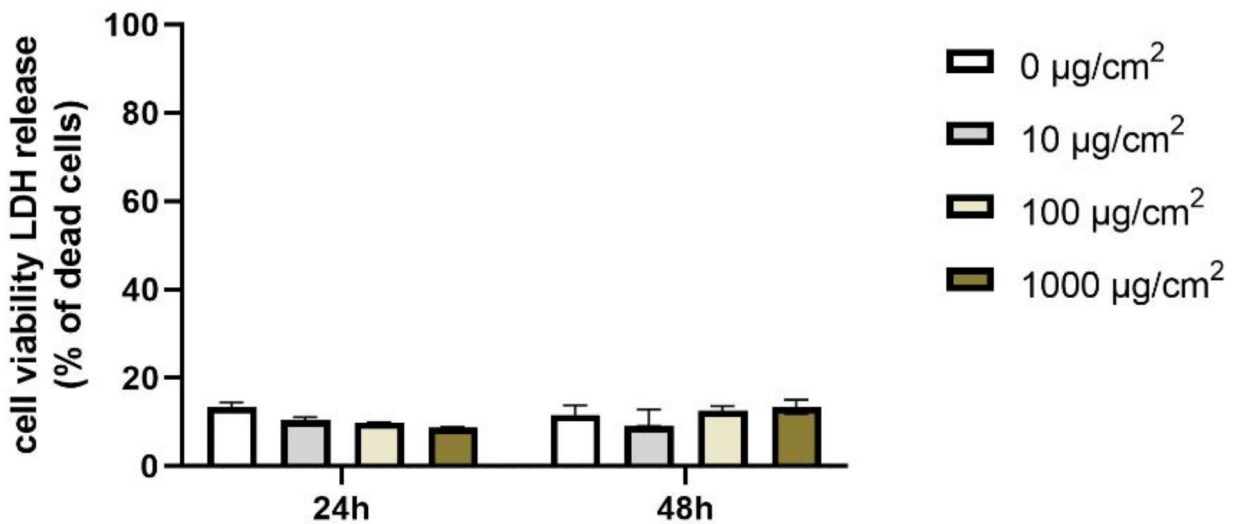


Fig. 3. Cell viability of human nasal epithelial cells exposed to different concentrations of microplastics (0, 10, 100, 1000 $\mu\text{g}/\text{cm}^2$) for 24 and 48 h. The data are presented as median (column) and interquartile range (IQR) (whiskers).

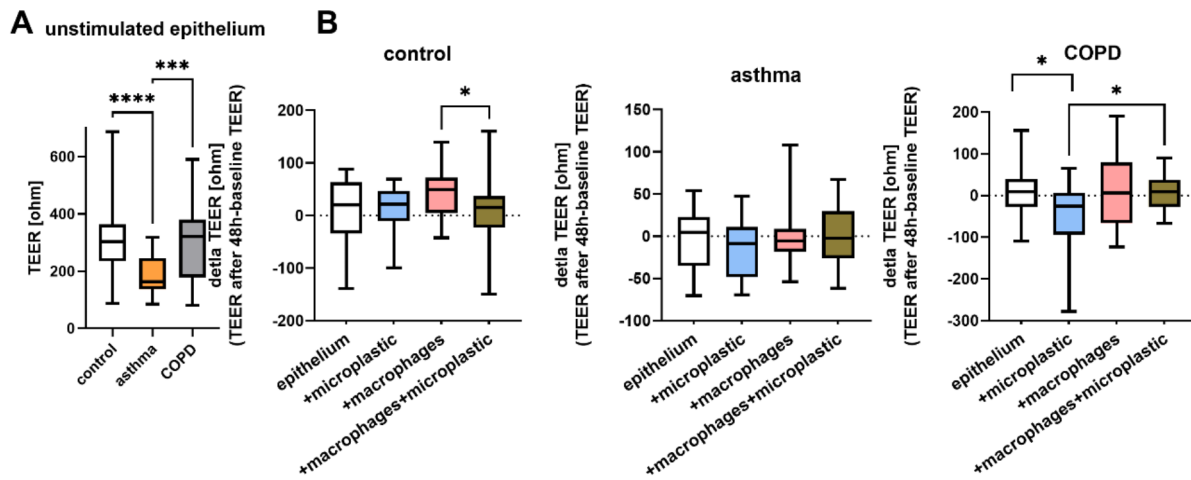


Fig. 4. Transepithelial electrical resistance (TEER) in untreated epithelial monocultures of control, asthma and COPD (A), TEER changes after 48 h of microplastic exposure in monocultures of epithelial cells and epithelial/macrophage co-cultures (B). The data are presented as median (line), IQR (box) and 5–95 percentile (whiskers). * $p \leq 0.05$; ** $p \leq 0.01$; *** $p \leq 0.001$; **** $p \leq 0.0001$.

epithelial cells in COPD (compared to controls) but increased number of secretory epithelial cells in asthma (compared to COPD).

The effect of polyamide fibres on the expression of CCR2, CD206, CD210, CD44, HLA-DR, TLR4 CD193, EGFR and TGF β on monocyte derived macrophages

Microplastic exposure decreased CCR2 expression and increased the expression of CD210 and TLR4 on monocyte-derived macrophages in controls (Fig. 9).

Number of genes with adjusted p-value <i>p</i> <0.05	The most significant DEGs in comparison of epithelium + microplastic vs. unstimulated epithelium (all three groups included)	Adjusted p-value	Fold change
199	PTPRH	0.0000000000002	1.63
	FBLN2	0.000003	0.79
	BCL2L15	0.000004	1.47
	BTG3	0.000006	1.19
	ANKRD36C	0.000006	1.38
	HCAR2	0.00002	0.78
	MAFF	0.00002	1.44
	DPP4	0.00004	0.68
	SCGB3A1	0.00004	0.70
	TUBA1B	0.00004	1.13
	FST	0.00004	1.38
	C15orf48	0.00004	1.47
	HMCN1	0.00004	0.77
	HMGCS1	0.0001	1.24
	CYBRD1	0.0001	0.83
	CAPN14	0.0002	1.45
	ZBTB16	0.0004	0.74
	ITPRIPL1	0.0004	0.73
	LINC00342	0.0004	1.37
	EPHX1	0.0005	0.83
	IDI1	0.0005	1.20
	FDPS	0.0005	1.20
	CLEC7A	0.0007	0.73
	IL19	0.0008	1.37
	PTPRQ	0.0009	0.78

Table 2. Differentially expressed genes (DEGs) (up and downregulated) in control, asthma and COPD groups related to microplastic exposure in nasal epithelial cells.

Discussion

The impact of microplastic particles on morbidity and the progression of lung diseases is not fully understood. This study aimed to assess the impact of polyamide fibres on the respiratory epithelium using an *in vitro* model, with a special focus on epithelial interactions with immune cells (macrophages) in obstructive lung diseases. For the first time, we described the processes caused by microplastic particles in asthma and COPD, which might be potential inducers of epithelial damage after microplastic inhalation. We found that 48-hour microplastic stimulation did not induce LDH release, a marker of cell viability and cause slight an inflammatory effect: it induced inflammatory cytokine secretion only for IL-8 production in controls (epithelial/ moMφs co-culture) and asthmatic (monoculture) epithelial cells. We selected the mediators of microplastic stimulation of epithelial cells in asthma and COPD. In COPD, the epithelial reaction to microplastic stimuli was significantly altered by macrophages. The epithelium of healthy controls responded differently; the expression of evaluated mediators was not changed in this group after microplastic stimulation. The upregulation of CD24 expression on ciliated epithelial cells, as well as CD193 and EGFR on basal epithelial cells, seemed to be an element of the epithelial response to microplastics in asthma. Polyamide particles downregulated the expression of CCR2 and upregulated CD210 and TLR4 on macrophages. Microplastic treatment disrupted the epithelial barrier in both control and COPD groups. The reaction of asthma and COPD epithelial cells to polyamide fibres is different than in controls due to disease-related epithelial reprogramming additionally impacted by macrophage response to hazardous environmental stimuli. Our study showed that 48-hour stimulation with polyamide particles is neutral for viability of nasal epithelial cells. Similar results were reported earlier by other authors^{41,42}. On the other hand, some papers suggested cytotoxic properties of microplastic particles (mainly polystyrene beads) in immortalized human bronchial epithelial cell lines (BEAS-2B, A549)⁸. It has been shown that frequent cell passages affect the characteristics of these cell lines, their response to stimuli, and protein expression that might be different than in primary cells⁴³. When discussing this, we should consider different types and concentration of plastic particles used by other authors. It is suggested that toxicity of microplastic particles is determined by their physical (size, shape, and concentration of particles), and chemical properties (chemical composition of monomers and chemical processing additives). The majority of studies assessing the *in vitro* cytotoxic effect of microplastics used polystyrene as commercially available particles, but polystyrene is not a common synthetic pollutant found in the air. In contrast, the prevalence of polyamide particles in the air is commonly reported as this type of plastic undergoes fragmentation, and its particles remain suspended in the air². It should be also be noted that here we report the short-term effect of sterile polyamide fibres on epithelial cells. The long-term

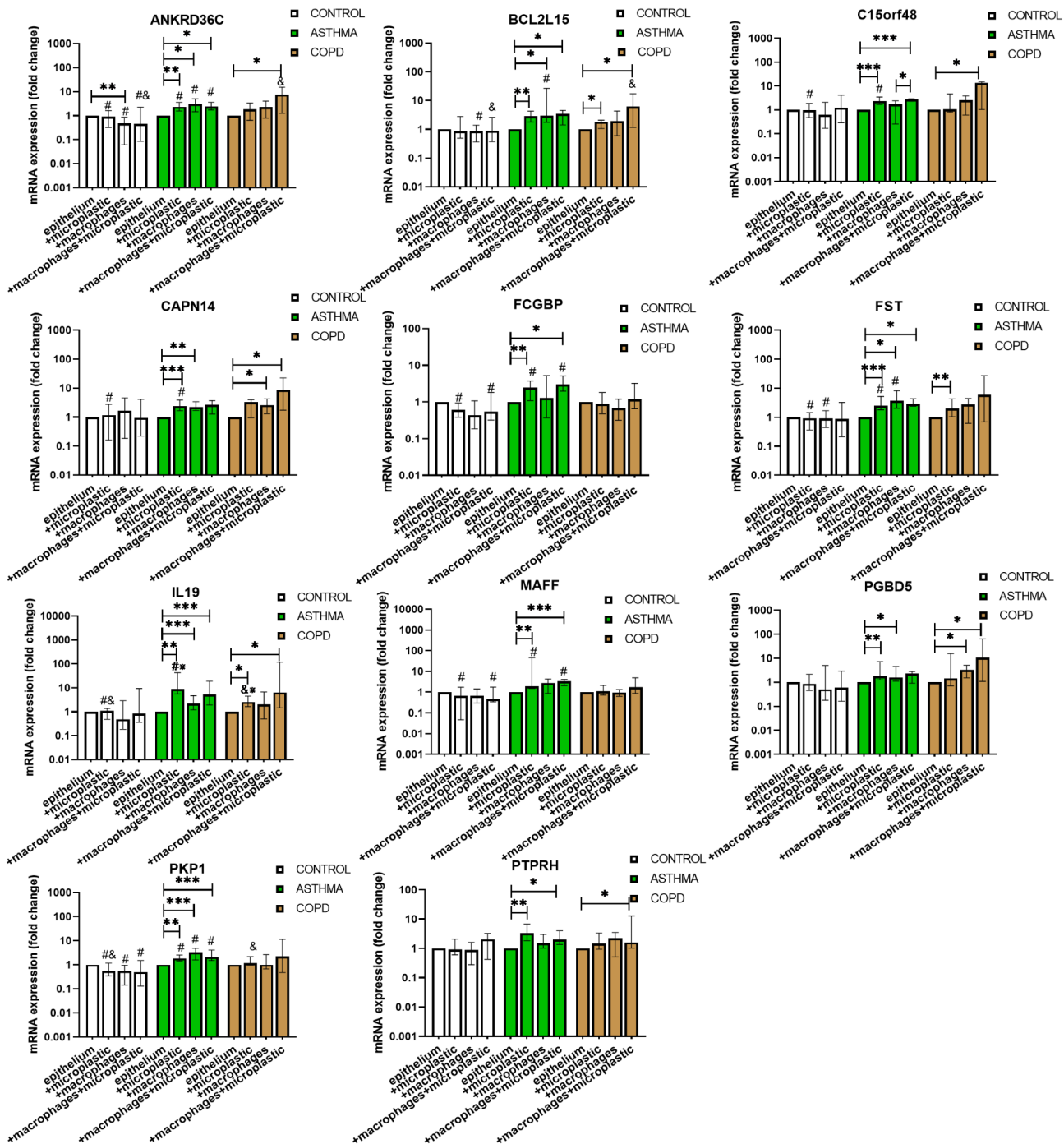


Fig. 5. mRNA expression of selected markers in epithelium after 48 h microplastic exposure in epithelial mono- and epithelial/macrophage co-cultures across control, asthma, and COPD groups. The data are shown as median (column) and interquartile range (IQR) (whiskers). * $p \leq 0.05$; ** $p \leq 0.01$; *** $p \leq 0.001$. ANKRD36 – ankyrin repeat domain 36, BCL2L15 – B-cell lymphoma 2 (Bcl-2)-like protein 15, C15orf48 – Chromosome 15 open reading frame 48, CAPN14 – calpain 14, FCGBP – IgGFc-binding protein, FST – follistatin, IL-19 – interleukin 19, MAFF – musculoaponeurotic fibrosarcoma oncogene homolog F, PGBD5 – piggyBac transposable element derived 5, PKP1 – plakophilin 1 and PTPRH – protein tyrosine phosphatase receptor type H.

stimulation and the influence of chemical-biological loads attached to air-derived microplastic fibres require further evaluation. On the other hand the method we chose for cell viability evaluation, based on LDH release – we found that nylon microparticles did not induce LDH release which is a marker of cell viability, but for the comprehensive assessment of the process the additional methodologies should be incorporated.

Biological Process

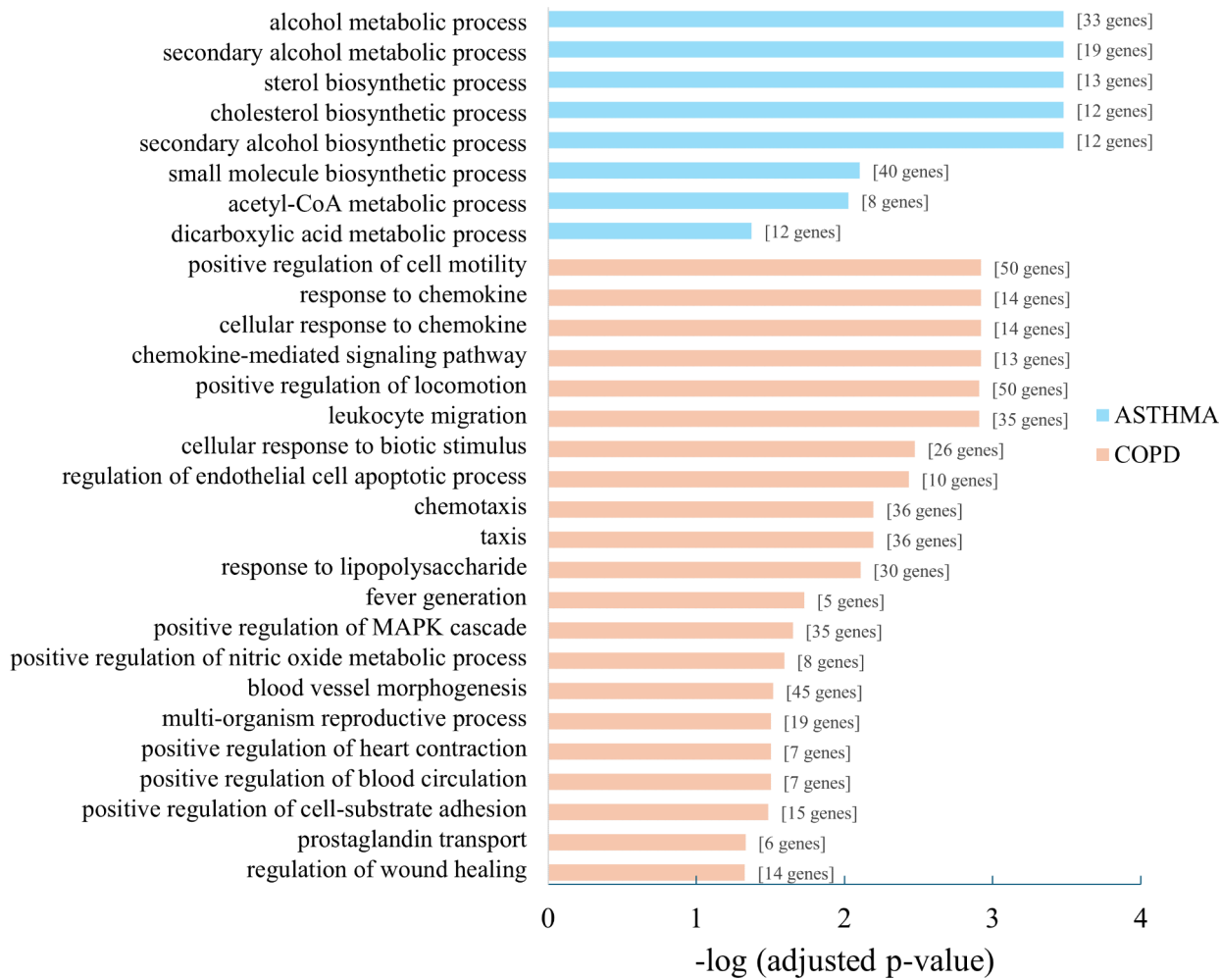


Fig. 6. Biological processes most significantly overrepresented among the top 5% of genes (based on the p-values) differentiated after microplastic exposure in epithelial monoculture.

As the respiratory epithelium is the first line of defence against inhaled pollutants, these cells secrete numerous inflammatory mediators to attract the immune cells and maintain a proper local, protective response. Epithelial cells from asthma and COPD patients produce higher amounts of inflammatory cytokines e.g., IL-6 or IL-8 as the pathobiology of these diseases is related to chronic local inflammation and elevated numbers of eosinophils (typically in asthma) or neutrophils (predominantly in COPD) in the lungs. The results of this study did not support the hypothesis of a pro-inflammatory effect of polyamide particles on either control or disease-affected airway epithelium. In contrast to PM_{2.5}, well characterized inflammation inducer that upregulated IL-6 and IL-8 secretion from epithelial cells⁴⁴, the levels of these cytokines was not changed by microplastic or macrophage co-stimulation. Other authors have reported a pro-inflammatory effect of polystyrene particles (upregulation of IL-6 expression) but only in immortalized cell line, not in primary epithelial cells⁴⁵. Similarly to ours results, Donkers et al. did not find increased secretion of IL-6 or IL-8 testing various plastics (polystyrene, polyethylene, nylon, car tire, and marine microplastic collected from the ocean) in advanced *in vitro* model of specialized respiratory epithelial cells (MucilAir)⁴⁶. The literature lacks reports comparing the asthma and COPD epithelial response to microplastic stimulation. An animal study with control and asthmatic mouse models demonstrated pulmonary inflammatory cell infiltration, bronchoalveolar macrophage aggregation, and increased TNF- α production in lungs of normal mice after microplastic exposure⁴⁷. Interestingly, Th2 cytokines were upregulated by microplastic only in asthmatic mice. In our work, the possible induction of a Th2 response in asthma after microplastic stimulation was observed as increased CD193 + expression on basal epithelial cells in asthma group. CD193 (CCR3) triggers Th2 inflammation associated with eosinophils signalling via eotaxins, which are strong eosinophil chemoattractants. More detailed studies are needed to explore this interesting finding.

We found that microplastic treatment impacted the integrity of epithelial barrier in two cases: in controls – decreased TEER values in epithelial- moMφs co-cultures and in COPD in epithelial monocultures. Our results suggest that co-cultivation of epithelial cells with macrophages protects the epithelial barrier in COPD against microplastic stimuli. We hypothesized that macrophages, together with epithelial cells, are key immune cells crucial for microplastic processing in the lungs. It seems that in healthy people, the 48-hour presence of microplastics alone on the surface of the epithelium did not disturb the cell barrier. However, when this

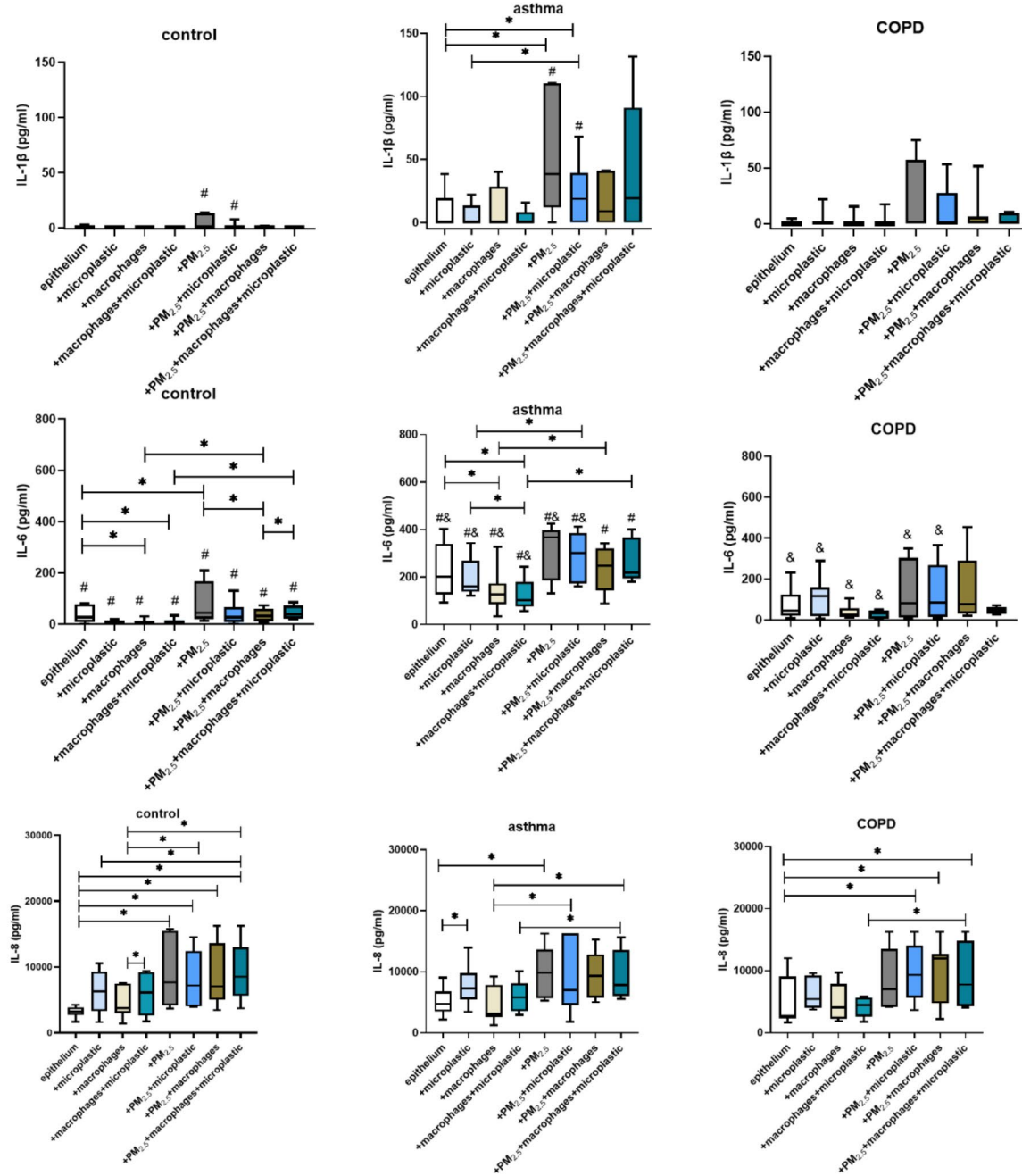


Fig. 7. IL-1 β , IL-6, and IL-8 secretion by epithelial mono- and epithelial/macrophage co-cultures in control, asthma, and COPD groups with or without microplastic and PM_{2.5} stimulation. Data are presented as median (line), IQR (box) and 5–95 percentile (whiskers). * $p \leq 0.05$; * $p \leq 0.05$; Wilcoxon signed-rank test. # - $p \leq 0.05$ in comparison control vs. asthma; & $p \leq 0.05$ in comparison COPD vs. asthma, Mann-Whitney test.

response included macrophages, the TEER values were lower, probably due to proteolytic proteins secreted by macrophages or epithelial cells in response to macrophage and microplastic stimuli. In COPD, due to structural epithelial changes related to disease pathobiology and dysfunction of macrophages, the epithelial response to microplastic stimuli is different. It has been suggested that possible disruption of epithelial barrier by microplastic might be caused by oxidative stress induced by this stimulation⁴⁸. Although we did not evaluate this parameter in our study, this hypothesis might be supported by results of similar research⁴⁸.

The analysis of RNA-Seq results revealed very interesting findings describing the pattern of epithelial response after microplastic exposure in asthma and COPD. The GO analysis demonstrated the diverse epithelial reaction to microplastic in both healthy individuals and those with obstructive lung diseases. This is consistent

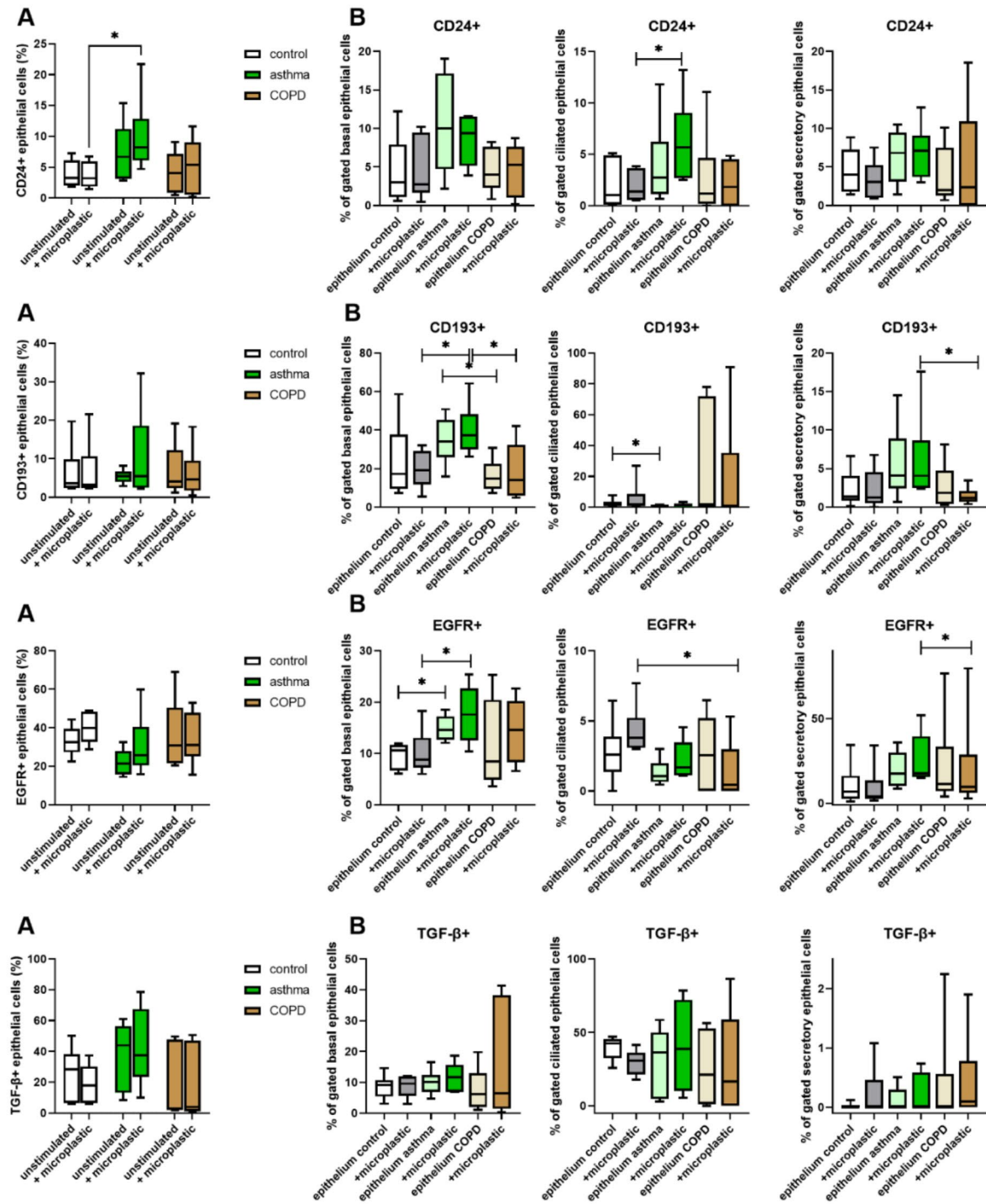


Fig. 8. CD24, CD193, EGFR, and TGF- β expression after microplastic treatment in epithelial cells (A), and in basal, ciliated, and secretory epithelial cells (B) of control, asthma, and COPD groups. Data are presented as median (line), IQR (box) and 5–95 percentile (whiskers). * $p \leq 0.05$.

with our previously published data, which characterized distinct biological processes in the nasal epithelium of patients with asthma and COPD compared to healthy controls after urban particulate matter exposure. These findings suggest genetic reprogramming of epithelium by ongoing pathophysiological processes in obstructive lung diseases⁴⁹. In this study, we pointed out the biological processes impacted by microplastic in asthma and COPD, whereas no differentially up and down regulated biological processes were found in controls. According

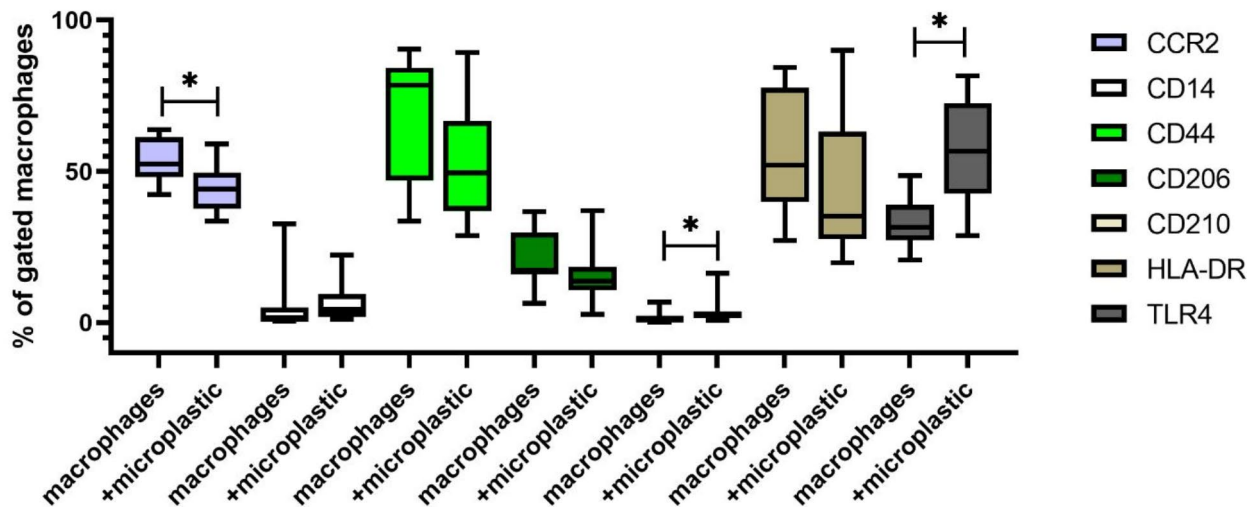


Fig. 9. CCR2, CD206, CD210, CD44, HLA-DR and TLR4 expression on moMφs after 48 h of microplastic stimulation in controls. Data are shown as median (column) and interquartile range (IQR) (whiskers). * $p \leq 0.05$; ** $p \leq 0.01$.

to our study, the potential damage to the asthmatic epithelial layer by microplastics is related to sterol, cholesterol and alcohol metabolism. The crucial role of sterols and oxysterols in asthmatic immune response has recently gained attention. Cholesterol is a component of surfactant⁵⁰. Additionally, dysfunction of lipid metabolism can contribute to inflammatory response in asthma. Fatty acids activate macrophage IL-1 β , IL-6 and TNF- α secretion⁵¹ and impact the macrophage M1 and M2 polarization⁵². ω 6 fatty acid-derived metabolites, such as leukotrienes and prostaglandins, have been shown to delay eosinophilic apoptosis⁵³. Lipid metabolism also regulates CD4+ T cells differentiation and activation⁵⁴. We found that important gene in asthmatic response to microplastic stimuli is ALCY. ALCY (ATP citrate lyase) promotes glycolysis, produces acetyl-CoA (AcCoA) from mitochondrial citrate for cholesterol and fatty acid biosynthesis. Ac-CoA is a crucial biosynthetic precursor, essential for the synthesis of fatty acids, cholesterol, and acetylcholine. ALCY-mediated cytoplasmic citrate metabolism is a very important mitochondrial pyruvate metabolism for regulation of basal cell differentiation in governance of epigenetic remodelling⁵⁵. Studies have demonstrated that long-term exposure to PM_{2.5} increased ALCY expression, which might be associated with epithelial-mesenchymal transition⁵⁶. The results of our study suggest, the response of asthmatic epithelial cells to microplastic exposure involves enhanced mitochondrial processes, utilizing extracellular carbon sources and lipid metabolic pathways mediated by ALCY.

GO analysis highlighted a classical inflammatory response, including chemokine release and leukocyte attraction into the airways and positive response of cell motility after microplastic exposure in COPD. We selected three most important genes from GO analysis associated with described terms: TREM2, CXCL8, and CX3CL1. Triggering receptor expressed on myeloid cells 2 (TREM2) plays a pivotal role in regulating the lipid handling capacities of pulmonary macrophages and triggering fibrosis. TREM2 is also a crucial mediator in macrophages during microbial acute infections. The soluble form of CX3CL1 is a known chemoattractant for monocytes, NK cells, and T cells. Its release requires the activity of the metalloproteinase ADAM10, which cleaves both the chemokine domain and the mucin-like stalk domain⁵⁷. The expression of CX3CL1 is induced by TNF- α , produced by monocytes, mast cells, and neutrophils in endothelial cells, thereby enhancing immune cell migration via the CX3CL1–CX3CR1 interaction⁵⁸. Our study indicated that microplastic stimulation in COPD epithelial cells initiates a cascade of reactions involving chemoattractants such as TREM2, CXCL8, and CX3CL1. This leads to the recruitment of monocytes, macrophages, and neutrophils to the airways, inflammation and potentially loosening of epithelial cell-cell interactions. Consequently, this process may positively regulate epithelial motility and locomotion, driving epithelial-mesenchymal transitions and contributing to carcinogenesis and fibrosis⁵⁹. To verify the role of selected genes in response of epithelial cells for microplastic stimuli the additional protein studies are required. Based on RNA-Seq results, we selected the best candidate genes of epithelial response in asthma and COPD for qPCR verification. Interestingly, genes activated in asthma are linked to three main biological responses: Th2 inflammation (IL-19, CAPN14)^{60,61}, stress-related genes associated with dampening of acute inflammation and cell protection (C15ORF48, PTPRH, FST, FCGBP)^{62–65}, and cancer (ANKRD36C, PGBD5, PKP-1, PTPRH, MAFF, FCGBP)^{66–70}. In COPD, some of these genes were also confirmed, including those related to Th2 inflammation (IL-19, CAPN14), stress-response genes associated with dampening of acute inflammation (C15ORF48, PTPRH, FST), cancer (ANKRD36C, PGBD5, PTPRH) in epithelial/macrophage co-cultures. The only exception was FST, whose expression was increased in epithelial monocultures only. This result suggests the significance of proper epithelial/macrophage interaction in response to microplastic stimuli. Macrophages and epithelial cells are crucial for maintaining lung homeostasis, efficient clearance of inhaled pathogens and air pollutants, as well as protective immune response. The interactions between these cells include

signal transduction via extracellular vesicles, communication mediated by cytokines and chemokines, and intercellular gap junction channels establishment⁷¹. In COPD, prolonged inflammation and oxidative stress lead to multiple cell dysfunctions, extracellular matrix proteolysis, and tissue injury. A detailed study of Sauler et al. using single cell RNA-Seq of lung tissue from COPD patients identified significant cell populations responsible for a disrupted stress response. These populations included a subpopulation of HHIP-expressing alveolar epithelial type II cells with decreased NUPR1 expression, endothelial cells with increased inflammatory CXCL-motif chemokine signalling and a subpopulation of high metallothionein-expressing alveolar macrophages⁷². The results of our study confirmed the importance of macrophage/epithelial interaction in COPD in response to microplastic stimuli.

We found that the macrophage response to microplastic exposure included the expression of CD210, TLR4, and CCR2. We suggest that macrophages recognize polyamide fibers via TLR4, which has been previously identified as an important indicator for microplastic action⁷³. The response of macrophages to microplastic stimuli appears to activate anti-inflammatory action regulated by IL-10 through CD210 activation as IL-10 is the only ligand for CD210. Additionally, the downregulation of CCR2, an important marker for monocyte recruitment and wound healing, after polyamide treatment, indicates the inflammatory reaction suppression by macrophages after this kind of treatment.

The results of our study clearly showed that neither cytotoxicity nor inflammation, but rather an immune response linked to Th2 inflammation, stress response, and especially carcinogenesis is a significant pathway altered by polyamide fibres in epithelial/macrophage co-cultures of asthma and COPD patients. Many of the gene candidates selected from RNA-Seq analysis are related to cancer (upregulated in many cancer types according to the literature), and the activation of CD24 on primarily ciliated asthmatic epithelial cells after microplastic stimulation further supports this theory. Although CD24 is normally expressed on epithelial cells, its upregulation has been shown to be crucial in tumor initiation, proliferation and metastasis⁷⁴. Our study indicated that asthmatic and COPD airway epithelial cells are more prone to carcinogenesis due to prolonged contact with inhaled microplastic fibres.

Our study has some limitations. Firstly, the use of bronchial epithelial cells would have been more informative for our purpose. However, the methodological restriction related to invasively obtaining bronchial tissue, especially from healthy individuals or those with highly reactive asthma, necessitated the use of non-invasively obtained nasal epithelial cells as a surrogate for bronchial epithelial cells. Secondly, we used weakly polarized macrophages without inducing M1, M2, or M10 polarization. Macrophage polarization is highly dependent on the cytokine environment in local tissue, and macrophages can easily change their polarization type when the cytokine profile varies. In this study we used a basic profile of monocyte derived macrophages as a starting point for further macrophage specialization after polyamide fibres treatment. We believe our results constitute an initial point of insights and serve as a foundation for future investigations into more detailed patterns of immune reactions. Thirdly, we did not include patients with severe asthma and COPD stages into our study because of the frequent oral steroid and antibiotic treatment in this group of patients, that can significantly affect epithelial cell immunology and be bias for evaluation of epithelial response to potentially harmful stimulation such as microplastic fibres.

Conclusions

This study demonstrated that asthmatic and COPD airway epithelial cells exhibit a different reaction to microplastic fibers stimulation compared to healthy epithelial cells. We found no cytotoxic and minor inflammatory effect of polyamide fibres on epithelial cells. Instead, the main significant response pattern is linked to Th2 inflammation, modulation of stress response, and, most notably, carcinogenesis. Our findings indicate that asthmatic and COPD epithelial cells are more vulnerable to cancer-related immune responses following microplastic inhalation and improper airway clearance. The structural impairment of the airway epithelium in obstructive diseases enhances the impact of microplastic particles compared to healthy epithelium.

Data availability

The RNA-Seq data were uploaded to GEO Omnibus (reference no. GSE273262). <https://www.ncbi.nlm.nih.gov/geo/query/acc.cgi?acc=GSE273262>.

Received: 5 September 2024; Accepted: 17 January 2025

Published online: 04 February 2025

References

- Zhu, L. et al. Tissue accumulation of microplastics and potential health risks in human. *Sci. Total Environ.* **915**, 170004 (2024).
- Wright, S. L., Ulke, J., Font, A., Chan, K. L. A. & Kelly, F. J. Atmospheric microplastic deposition in an urban environment and an evaluation of transport. *Environ. Int.* **136**, 105411 (2020).
- Bakand, S., Hayes, A. & Dechsakulthorn, F. Nanoparticles: A review of particle toxicology following inhalation exposure. *Inhal Toxicol.* **24**, 125–135 (2012).
- Carvalho, T. C., Peters, J. I. & Williams, R. O. Influence of particle size on regional lung deposition—what evidence is there? *Int. J. Pharm.* **406**, 1–10 (2011).
- Donaldson, K. & Tran, C. L. Inflammation caused by particles and fibers. *Inhal Toxicol.* **14**, 5–27 (2002).
- Yacobi, N. R. et al. Nanomaterial interactions with and trafficking across the lung alveolar epithelial barrier: Implications for health effects of air-pollution particles. *Air Qual. Atmos. Health* **4**, 65–78 (2011).
- Ultrafine particles cross. Cellular membranes by nonphagocytic mechanisms in lungs and in cultured cells - PubMed. <https://pubmed.ncbi.nlm.nih.gov/16263511/>
- Dong, C. D. et al. Polystyrene microplastic particles: In vitro pulmonary toxicity assessment. *J. Hazard. Mater.* **385**, 121575 (2020).

9. Kelly, F. J. & Fussell, J. C. Air pollution and public health: Emerging hazards and improved understanding of risk. *Environ. Geochem. Health.* **37**, 631–649 (2015).
10. Paget, V. et al. Specific uptake and genotoxicity induced by polystyrene nanobeads with distinct surface chemistry on human lung epithelial cells and macrophages. *PLoS One.* **10**, e0123297 (2015).
11. Jiang, X. Q., Mei, X. D. & Feng, D. Air pollution and chronic airway diseases: What should people know and do? *J. Thorac. Dis.* **8**, E31–40 (2016).
12. 2023 GINA Main Report. *Global Initiative for Asthma - GINA* <https://ginasthma.org/2023-gina-main-report/>
13. 2023, G. O. L. D. & Report Global Initiative for Chronic Obstructive Lung Disease - GOLD <https://goldcopd.org/2023-gold-report-2/>
14. Cole, M. A novel method for preparing microplastic fibers. *Sci. Rep.* **6**, 34519 (2016).
15. Paplinska-Goryca, M. et al. Interactions of nasal epithelium with macrophages and dendritic cells variously alter urban PM-induced inflammation in healthy, asthma and COPD. *Sci. Rep.* **11**, 13259 (2021).
16. Bolger, A. M., Lohse, M. & Usadel, B. Trimmomatic: A flexible trimmer for Illumina sequence data. *Bioinformatics* **30**, 2114–2120 (2014).
17. Kim, D., Langmead, B. & Salzberg, S. L. HISAT: A fast spliced aligner with low memory requirements. *Nat. Methods* **12**, 357–360 (2015).
18. McKenna, A. et al. The genome analysis Toolkit: A MapReduce framework for analyzing next-generation DNA sequencing data. *Genome Res.* **20**, 1297–1303 (2010).
19. Li, H. et al. The sequence Alignment/Map format and SAMtools. *Bioinformatics* **25**, 2078–2079 (2009).
20. Quast, C. et al. The SILVA ribosomal RNA gene database project: Improved data processing and web-based tools. *Nucleic Acids Res.* **41**, D590–596 (2013).
21. Kopylová, E., Noé, L. & Touzet, H. SortMeRNA: Fast and accurate filtering of ribosomal RNAs in metatranscriptomic data. *Bioinformatics* **28**, 3211–3217 (2012).
22. Zerbino, D. R. et al. Ensembl 2018. *Nucleic Acids Res.* **46**, D754–D761 (2018).
23. Anders, S., Pyl, P. T. & Huber, W. HTSeq—a Python framework to work with high-throughput sequencing data. *Bioinformatics* **31**, 166–169 (2015).
24. Love, M. I., Huber, W. & Anders, S. Moderated estimation of Fold change and dispersion for RNA-seq data with DESeq2. *Genome Biol.* **15**, 550 (2014).
25. Zhu, A., Ibrahim, J. G. & Love, M. I. Heavy-tailed prior distributions for sequence count data: Removing the noise and preserving large differences. *Bioinformatics* **35**, 2084–2092 (2019).
26. The Gene Ontology Consortium. The gene ontology resource: 20 years and still GOing strong. *Nucleic Acids Res.* **47**, D330–D338 (2019).
27. Kanehisa, M., Furumichi, M., Tanabe, M., Sato, Y. & Morishima, K. KEGG: New perspectives on genomes, pathways, diseases and drugs. *Nucleic Acids Res.* **45**, D353–D361 (2017).
28. Yu, G., Wang, L. G., Han, Y. & He, Q. Y. clusterProfiler: An R package for comparing biological themes among gene clusters. *OMICS* **16**, 284–287 (2012).
29. Bonser, L. R. et al. Flow-cytometric analysis and purification of airway epithelial-cell subsets. *Am. J. Respir Cell. Mol. Biol.* **64**, 308–317 (2021).
30. Wojnacki, J. et al. Tetraspanin-8 sequesters syntaxin-2 to control biphasic release propensity of mucin granules. *Nat. Commun.* **14**, 3710 (2023).
31. Siddiqui, S. et al. Epithelial miR-141 regulates IL-13-induced airway mucus production. *JCI Insight* **6**, e139019–e139019 (2021).
32. Kawakita, K. et al. Role of basal cells in nasal polyp epithelium in the pathophysiology of eosinophilic chronic rhinosinusitis (eCRS). *Allergol. Int.* **73**, 563–572 (2024).
33. Ganeshan, S. & Sajjan, U. S. Repair and remodeling of airway epithelium after injury in Chronic Obstructive Pulmonary Disease. *Curr. Respir. Care Rep.* **2**, (2013).
34. Beck, L. A. et al. Functional analysis of the chemokine receptor CCR3 on airway epithelial cells. *J. Immunol.* **177**, 3344–3354 (2006).
35. Yang, Y., Zhu, G., Yang, L. & Yang, Y. Targeting CD24 as a novel immunotherapy for solid cancers. *Cell. Commun. Signal.* **21**, 312 (2023).
36. Puchowicz, D., Cieslak, M., Puchowicz, D. & Cieslak, M. Raman spectroscopy in the analysis of textile structures. in *Recent Developments in Atomic Force Microscopy and Raman Spectroscopy for Materials Characterization* IntechOpen, (2021). <https://doi.org/10.5772/intechopen.99731>
37. Milani, A. Unpolarized and polarized Raman spectroscopy of nylon-6 polymorphs: A quantum chemical approach. *J. Phys. Chem. B.* **119**, 3868–3874 (2015).
38. Miller, J. V. & Bartick, E. G. Forensic analysis of single fibers by Raman Spectroscopy. *Appl. Spectrosc.* **55**, 1729–1732 (2001).
39. Uematsu, H. et al. Relationship between crystalline structure of polyamide 6 within carbon fibers and their mechanical properties studied using Micro-raman spectroscopy. *Polymer* **223**, 123711 (2021).
40. Song, K. & Rabolt, J. F. Polarized Raman measurements of Uniaxially oriented poly(ϵ -caprolactam). *Macromolecules* **34**, 1650–1654 (2001).
41. Stock, V. et al. Uptake and cellular effects of PE, PP, PET and PVC microplastic particles. *Toxicol. Vitro.* **70**, 105021 (2021).
42. Annangi, B. et al. Effects of true-to-life PET nanoplastics using primary human nasal epithelial cells. *Environ. Toxicol. Pharmacol.* **100**, 104140 (2023).
43. Sambuy, Y. et al. The Caco-2 cell line as a model of the intestinal barrier: Influence of cell and culture-related factors on Caco-2 cell functional characteristics. *Cell. Biol. Toxicol.* **21**, 1–26 (2005).
44. Zou, W. et al. PM2.5 induces the expression of inflammatory cytokines via the Wnt5a/Ror2 pathway in human bronchial epithelial cells. *Int. J. Chron. Obstruct. Pulmon. Dis.* **15**, 2653–2662 (2020).
45. Yang, S. et al. In vitro evaluation of nanoplastics using human lung epithelial cells, microarray analysis and co-culture model. *Ecotoxicol. Environ. Saf.* **226**, 112837 (2021).
46. Donkers, J. M. et al. Advanced epithelial lung and gut barrier models demonstrate passage of microplastic particles. *Microplastics Nanoplastics*, **2**, 6 (2022).
47. Lu, K. et al. Detrimental effects of microplastic exposure on normal and asthmatic pulmonary physiology. *J. Hazard. Mater.* **416**, 126069 (2021).
48. Zeng, G. et al. Polystyrene microplastic-induced oxidative stress triggers intestinal barrier dysfunction via the NF- κ B/NLRP3/IL-1 β /MCLK pathway. *Environ. Pollut.* **345**, 123473 (2024).
49. Misiukiewicz-Stepien, P. et al. RNA-Seq analysis of UPM-Exposed epithelium co-cultivated with macrophages and dendritic cells in Obstructive Lung diseases. *Int. J. Mol. Sci.* **23**, 9125 (2022).
50. Keating, E. et al. Effect of cholesterol on the biophysical and physiological properties of a clinical pulmonary surfactant. *Biophys. J.* **93**, 1391–1401 (2007).
51. Zhang, Q. et al. Fatty acid oxidation contributes to IL-1 β secretion in M2 macrophages and promotes macrophage-mediated tumor cell migration. *Mol. Immunol.* **94**, 27–35 (2018).
52. Morgan, P. K. et al. Macrophage polarization state affects lipid composition and the channeling of exogenous fatty acids into endogenous lipid pools. *J. Biol. Chem.* **297**, 101341 (2021).

53. Profita, M. et al. Increased prostaglandin E2 concentrations and cyclooxygenase-2 expression in asthmatic subjects with sputum eosinophilia. *J. Allergy Clin. Immunol.* **112**, 709–716 (2003).
54. Wang, R. et al. The transcription factor Myc controls metabolic reprogramming upon T lymphocyte activation. *Immunity* **35**, 871–882 (2011).
55. Li, Y. et al. Mitochondrial pyruvate carriers control airway basal progenitor cell function through glycolytic-epigenetic reprogramming. *Cell. Stem Cell.* **S1934-5909** (24), 00329–00321. <https://doi.org/10.1016/j.stem.2024.09.015> (2024).
56. Fu, Y. et al. Inhibition of ATP citrate lyase (ACLY) protects airway epithelia from PM2.5-induced epithelial-mesenchymal transition. *Ecotoxicol. Environ. Saf.* **167**, 309–316 (2019).
57. Schwarz, N. et al. Requirements for leukocyte transmigration via the transmembrane chemokine CX3CL1. *Cell. Mol. Life Sci.* **67**, 4233–4248 (2010).
58. Wolf, E. M., Fingleton, B. & Hasty, A. H. The therapeutic potential of TREM2 in cancer. *Front. Oncol.* **12**, 984193 (2022).
59. Hao, W., Li, M., Zhang, C., Zhang, Y. & Du, W. Increased levels of inflammatory biomarker CX3CL1 in patients with chronic obstructive pulmonary disease. *Cytokine* **126**, 154881 (2020).
60. Weng, Y. H., Chen, W. Y., Lin, Y. L., Wang, J. Y. & Chang, M. S. Blocking IL-19 signaling ameliorates Allergen-Induced Airway inflammation. *Front. Immunol.* **10**, 968 (2019).
61. Boruk, M. et al. Elevated levels of calpain 14 in nasal tissue in chronic rhinosinusitis. *ERJ Open. Res.* **6**, 00137–02020 (2020).
62. Takakura, Y. et al. Mitochondrial protein C15ORF48 is a stress-independent inducer of autophagy that regulates oxidative stress and autoimmunity. *Nat. Commun.* **15**, 953 (2024).
63. Chen, F. J. et al. PTPRH alleviates airway obstruction and Th2 inflammation in Asthma as a protective factor. *J. Asthma Allergy* **15**, 133–144 (2022).
64. Lin, C. et al. Transcriptional activation of follistatin by Nrf2 protects pulmonary epithelial cells against silica nanoparticle-induced oxidative stress. *Sci. Rep.* **6**, 21133 (2016).
65. Liu, Q. et al. Role of the mucin-like glycoprotein FCGBP in mucosal immunity and cancer. *Front. Immunol.* **13**, 863317 (2022).
66. Iqbal, Z. et al. Integrated genomic analysis identifies ANKRD36 gene as a novel and common biomarker of disease progression in chronic myeloid leukemia. *Biology (Basel)* **10**, 1182 (2021).
67. Henssen, A. G. et al. PGBD5 promotes site-specific oncogenic mutations in human tumors. *Nat. Genet.* **49**, 1005–1014 (2017).
68. Martin-Padron, J. et al. Plakophilin 1 enhances MYC translation, promoting squamous cell lung cancer. *Oncogene* **39**, 5479–5493 (2020).
69. Wang, S. et al. PTPRH promotes the progression of non-small cell lung cancer via glycolysis mediated by the PI3K/AKT/mTOR signaling pathway. *J. Transl Med.* **21**, 819 (2023).
70. Deng, Y. et al. The role and regulation of maf proteins in cancer. *Biomark. Res.* **11**, 17 (2023).
71. Bissonnette, E. Y., Lauzon-Joset, J. F., Debley, J. S. & Ziegler, S. F. Cross-talk between Alveolar macrophages and Lung epithelial cells is essential to maintain lung homeostasis. *Front. Immunol.* **11**, 583042 (2020).
72. Sauler, M. et al. Characterization of the COPD alveolar niche using single-cell RNA sequencing. *Nat. Commun.* **13**, 494 (2022).
73. Kwabena Danso, I., Woo, J. H., Baek, H., Kim, S., Lee, K. & K. & Pulmonary toxicity assessment of polypropylene, polystyrene, and polyethylene microplastic fragments in mice. *Toxicol. Res.* **40**, 313–323 (2024).
74. Wang, Y. et al. CD24 blockade as a novel strategy for cancer treatment. *Int. Immunopharmacol.* **121**, 110557 (2023).

Acknowledgements

The authors would like to thank Dr. Elwira Zajusz-Zubek for providing environmental samples.

Author contributions

MPG: Writing – original draft, Supervision, Methodology, Investigation, Funding acquisition, Conceptualization. PMS: Methodology, Investigation, Writing – review & editing, DA, JR, MK, MW, KMRz: Methodology, Writing – review & editing, KG: Methodology, Data curation. RK: Formal analysis, Writing – review & editing.

Funding

The study was granted from Jakub Potocki Foundation, Warsaw, Poland (5FJP01).

Declarations

Competing interests

RK reports personal fees and other from Boehringer Ingelheim, personal fees and other from Chiesi, personal fees and other from AstraZeneca, personal fees from Polpharma, outside the submitted work. The other authors declare no conflict of interest.

Ethics approval

All procedures performed in this study were in accordance with the ethical standards of the institutional and/or national research committee and with the 1964 Helsinki declaration and its later amendments or comparable ethical standards. This work has received approval for research ethics from Medical University of Warsaw Review Board (KB/30/2022) and a proof/certificate of approval is available upon request.

Additional information

Supplementary Information The online version contains supplementary material available at <https://doi.org/10.1038/s41598-025-87242-x>.

Correspondence and requests for materials should be addressed to M.P.-G.

Reprints and permissions information is available at www.nature.com/reprints.

Publisher's note Springer Nature remains neutral with regard to jurisdictional claims in published maps and institutional affiliations.

Open Access This article is licensed under a Creative Commons Attribution-NonCommercial-NoDerivatives 4.0 International License, which permits any non-commercial use, sharing, distribution and reproduction in any medium or format, as long as you give appropriate credit to the original author(s) and the source, provide a link to the Creative Commons licence, and indicate if you modified the licensed material. You do not have permission under this licence to share adapted material derived from this article or parts of it. The images or other third party material in this article are included in the article's Creative Commons licence, unless indicated otherwise in a credit line to the material. If material is not included in the article's Creative Commons licence and your intended use is not permitted by statutory regulation or exceeds the permitted use, you will need to obtain permission directly from the copyright holder. To view a copy of this licence, visit <http://creativecommons.org/licenses/by-nc-nd/4.0/>.

© The Author(s) 2025